NUMERICAL AND EXPERIMENTAL INVESTIGATION FOR MELTING BEHAVIOR OF PHASE CHANGE MATERIAL IN THE ANNULUS OF TWO CONCENTRIC PIPES

Mustafa B. Al-hadithi[1*], Saad. M. Jalil[1**]

[1]College of Engineering, University of Anbar, Anbar-Iraq

*mustafaalhadithi@uoanbar.edu.iq,** saad.jalil@uoanbar.edu.iq

The study analyzed numerically and experimentally the thermal performance and temperature evolution during the period of melting case of a Phase Change Material PCM inside an annular space of concentric pipes. The inlet temperature of the working fluid, water, that flows to the inner pipe of the annulus was maintained at almost a constant temperature of 333 K higher than the melting point of the PCM. The mathematical model for the current 3D coupled system was solved numerically by ANSYS FLUENT 2021 R1. The temperature at different positions in the system was measured under different mass flow rates. The preliminary results indicated that there is a very good matching and agreement between the computational and the experimental findings relating to the temperature measurements. Different mass flow rate cases are considered in the experiments ranging from 0.0952 kg/s to 0.0134 kg/s. This range of flow rates was utilized in running the experiments to obtain the required data. The results showed that there is a maximum variation, ranging from 3.4% to 4.8%, between the numerical and experimental findings at the maximum mass flow rate. This error is an acceptable limit for comparing the computational and experimental results in the present investigation.

Keywords *PCM, melting process, heat transfer fluid, finite volume method, paraffin wax*

1. Introduction.

The world is now in a state of rapid and continuous development of the economy, increasing energy consumption and demand has become a problem facing governments. Therefore, the problem of energy shortage becomes serious especially from early morning until after midday due to commercial, industrial, and residential activities during that period. There are two possible solutions to this problem. The first one is to shift the use of electricity from the peak period to the off-peak period. The second solution is recovering energy that is dissipated to the environment as waste heat, such as heat from an air conditioner condenser, or to collect and use thermal energy that fluctuates during the day such as solar energy. For this reason, it is necessary to provide an energy storage system.

A simple numerical method, called the temperature and thermal resistance iteration method, was developed by Long Jian-you [1]. This method is developed to analyze the melting and solidification of the PCM in three concentric tubes. The middle annulus is filled with PCM. In the charging period, the hot fluid flows in the outer channel, and the cold fluid flows inside the inner channel during the discharging process. This method is efficiently employed in simulating the charging and discharging

processes of the latent thermal energy storage unit. The numerical and experimental findings showed a good agreement.

Abduljalil A. Al-Abidi, *et al.* [2], a numerical investigation studied the interpretation of the solidification process in a heat exchanger of three tubes under the effect of internal and external fins to improve the heat transfer rates during the melting and solidification processes. In his study, the researcher reached different design parameters that affect the process of improving heat transfer. The simulation results show that these parameters had a significant effect on the freezing time of PCM completely. The effect of fin thickness was smaller than the fin length. The number of fins showed the same effect for solidification time as the number of PCM geometries. The results of the respective model showed acceptable agreement with experimental results except at the end of freezing where the temperature decrease in the experimental curves was greater than that of the numerical model.

Transient two-dimensional PCM physical model and one-dimensional heat transfer fluid HTF physical model were developed by Wei-Wei Wang, et al. [3]. The thermal performances of the phase change thermal energy storage PCTES under different mass flow rates of HTF and different HTF inlet temperatures. Also, the differences in the performances of PCTES under charging and discharging conditions are addressed. The study verified that the change of the temperature of the PCM during the charging and discharging processes has three phases related to the rate of heat charge or discharge: the fast-change period, the slowly changing period, and the slow-change period. They discovered in their work, that the mass flow rate of the heat transfer fluid has a small impact on the stored amount of energy, whereas in the charging or discharging period, it has a noticeable effect. Also, the required time to complete these two main processes decreases non-linearly as the flow rate of the heat transfer fluid increases.

Numerical and experimental investigation of the phase change process that is predominantly conductive heat transfer in thermal storage units is presented in [4]. The paraffin wax, as a PCM, is used as thermal energy storage by filling the space in the shell and tube type heat exchanger. A detailed parametric study was performed for various flow parameters and system dimensions such as different mass flow rates, HTF inlet temperatures, pipe thickness, and radius. The results indicated that the inlet HTF temperature has a significant impact on the charging and discharging PCM processes. However, there is no noticeable effect on the mass flow rate. Also, it is shown that the tube thickness is not a primary parameter for optimizing storage performance unit but the radius of the tube has a greater influence in terms of run time and storage unit outlet temperature.

Rathod, and Banerjee [5] used paraffin wax melting around 58-60 °C inside a heat exchanger to analyze the energy storage by the latent heat. The temperature evolution in a phase-change material was measured with time. The results indicate that the fluid inlet temperature has a greater effect on the heat fraction, which represents the ratio of input or output energy to the stored or released energy, compared to the HTF mass flow rate which affects the melting period. The results showed that the solidification process requires about 50% extra time to maintain a unity heat fraction compared with the melting process. Also, the required time for the PCM melting period increases with decreasing Reynolds number and the inlet temperature of the heat transfer working fluid.

A comprehensive characterization of paraffin wax as PCM is performed by Jaume Gasia, *et al*., [6] based on two different methods. The first method is laboratory characterization (mass range in mg) and the second method is analysis in a pilot plant (mass range in kg). The laboratory analysis showed suitability up to 80 °C and 1200 cycles. In the experimental plant analysis, the thermal behavior in a

shell and tube heat exchanger under different flow rates of the mass of the HTF was analyzed in terms of temperatures, power, and energy. The results showed no health risks, with a phase change temperature range of 50-61 °C and an enthalpy of 120.11 kJ/kg. Thermal stability and cycling tests have shown that this paraffin is suitable for use up to 80°C and causes no deterioration after 1200 cycles. Differences observed between charging and discharging are mainly due to the prevailing heat transfer mechanisms; mainly convection during the charging process, and mainly conduction during the discharging process.

In the study by Seddegh, S., *et al*. [7], the influence of engineering and operational parameters on cylindrical shell and tube latent heat thermal energy storage LHTES systems was investigated. Four different shell-to-tube radius ratios are considered with PCM on the casing side and HTF flowing through the tube. The results showed that the shell-to-tube radius ratio of 5.4 offers better system performance in terms of charging time and energy stored in the studied LHTES systems. It is found from the discharge process with HTF temperature of 10°C that after being charged with HTF at 70 °C and 80 °C, the temperature of PCM decreases rapidly and the temperature of change of HTF does not significantly affect the discharge process. Furthermore, it is also found that when all PCM is melted, the effect of natural convection decreases and thus reduces heat transfer between the HTF liquid and the PCM liquid.

The melting process of PCM with a constant ratio of the volume-mass fraction was modeled numerically in [8] with various arrangements of shell-and-tube energy storage system. The simulation showed the importance of natural convection on the amount of storage of latent energy for 3D pipe and cylinder simulation by FLUENT software. Computational results showed that free convection can lead to an unequal distribution in the interface of the solid-liquid region. This effect will accelerate the melting of the PCM. As a result of numerical solutions, it was concluded in the study that the thermal energy storage process can be divided into three stages; the sensible heat thermal energy storage stage, the LHTES takes place stage, and the PCM dissolving stage.

An investigation into the impact of varying the shell-to-tube radius ratio on the charging and discharging processes was conducted within a vertical shell-and-tube Latent Heat Thermal Energy Storage LHTES system, as detailed in reference [9]. This study encompassed two different series of geometrical configurations, each characterized by two unit heights. Also, the study showed that as the unit height increases, the charging process indicates a slight decrease in the optimal radius ratio. Whereas, the discharging process exhibits no substantial variation. The unit height's impact on the choice of the optimal radius ratio is minimal. The findings indicated that the thermal behavior is consistent across both examined series. An optimal radius ratio has been determined to be approximately equal to 5. This determination was based on assessing energy storage for a charging duration ranging from 6 to 8 hours and a discharging duration ranging from 15 to 20 hours. An isothermal inner pipe surface and an adiabatic outer shell surface of the annulus boundary conditions have been considered in [10]. The study showed that the rate of charging in the upper section of the shell is faster when contrasted with other areas. This acceleration is caused by the buoyancy-driven convection, which is intensified due to the expansion of the melted zone. Also, over a certain duration, the melting reaction of the PCM decelerates significantly. This phenomenon occurs because the melting temperature gradually aligns with the temperature of the inner tube surface, consequently diminishing the rate of heat transmission. Researchers have observed that the upper zone of the phase

change material exhibits a faster melting rate compared to the lower zone. Over 16 hours, temperature fluctuations near the pipe's outer surface reached a maximum of 43.75% and a minimum of 31.25%.

The current study aims to evaluate and analyze the duration required for the melting process of phase change material PCM within the annular geometry of horizontal double-pipe heat exchangers. This study reviews experimentally and numerically the transient thermal performance of PCM during the charging operation. Also, discussing the applicability of using it in thermal storage units within solar collectors and heat exchangers. The work investigates how the PCM material properties behave when it is employed in solar collectors, focusing on this specific application. The main goal of the present work is to elaborate on the interest in the Phase Change Material melting process to be used in storage units. Moreover, the study raises a question about how PCM can be used in domestic and industrial services compared to traditional collectors. The study will be carried out under various effective parameters.

2. Numerical Approach

2.1. Modeling and Governing Equations

The computational fluid dynamics CFD commercial software FLUENT (ANSYS 2021 R1) was used in modeling the PCM melting process. The governing equations were solved by the control volume method and by applying the Patankar SIMPLE algorithm. The convergence scales were set to 10^{-6} for all governing equations except for the energy equation was set to 10^{-6} with 10^{-3} seconds as a time step size to achieve a stable converged solution [11,12]. The two-equation pressure-based SST k-ω viscous turbulent model is employed for the closure of the RANS equations [13]. The melting model was considered for the PCM domain. Therefore, the governing Equations 1, 2, and 3 are as follows [11-13],

$$\frac{\partial \rho}{\partial t} + \nabla.(\rho u) = 0 \quad (1)$$

$$\frac{\partial}{\partial t}(\rho u) + \nabla.(\rho u u) = -\nabla \mathrm{p} + \nabla(\tau) + \rho \mathrm{g} + \mathrm{F} \quad (2)$$

$$\frac{\partial}{\partial t}(\rho H) + \nabla.(\rho u H) = \nabla(\mathrm{k}\nabla \mathrm{T}) + \mathrm{S} \quad (3)$$

Where H is the total enthalpy, τ is the stress tensor, ρg is the gravitational force, F is the body force, p is the pressure, t is the time, S is the source term and u is the velocity vector.

2.2. Computational Domain and Meshing

The numerical model is developed to be identical to the physical model in the experiments. Four domains are created in the computational model to be analyzed in the simulation: water, inner pipe, PCM, and outer pipe domains. The geometry is generated by ANSYS Design Modeler with dimensions matching the experimental counterpart scales as shown in Fig. 1. The ANSYS Meshing 2021R1 software is used in the mesh discretization by applying the Finite Volume Method as shown in Fig. 2. The PCM and tubes domains are generated from a structured mesh, whereas, most of the water

domain was represented with tetrahedral and hexahedral elements. The properties of the computational domains that are used in this analysis are given in Tables 1, 2, and 3.

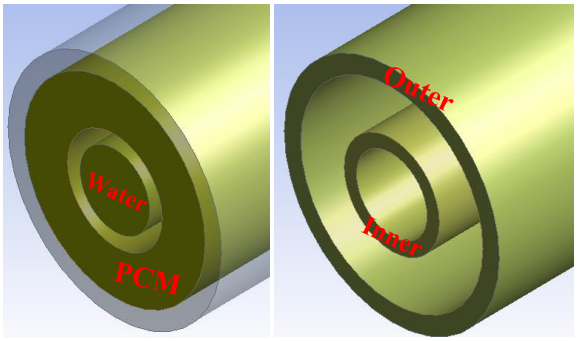

Figure 1 Physical Domains

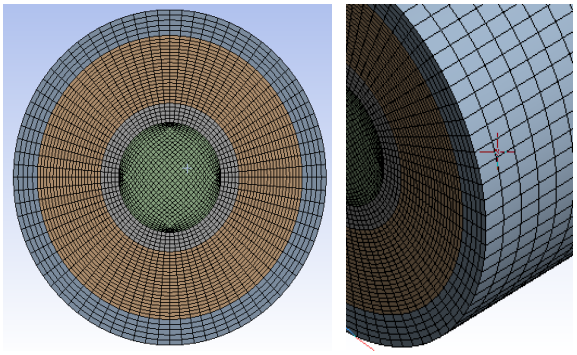

Figure 2 Enlarged isometric section front view of the considered Mesh

Table: 1 Paraffin wax Thermophysical properties [14].	
Melting Temperature	50^0 C
Liquid State Density	790 kg/m^3
Solid State Density	910 kg/m^3
Liquid State Specific heat	2150 J/kg.K
Solid State Specific heat	2000 J/kg.K
Latent Heat	190000 J/kg
Liquid State Thermal conductivity	0.22 W/m.K
Solid State Thermal conductivity	0.24 W/m.K
Kinematic viscosity	$5.2*10^{-6}$ m^2/s
Dynamic viscosity (liquid state)	$4.108*10^{-3}$ N.s/m^2
Dynamic viscosity (Solid state)	$4.732*10^{-3}$ N.s/m^2

Table 3 Water properties [15].	
Water at (24^0 C)Density	997 kg/m^3
Thermal conductivity	0.613 W/m.K
Specific heat	4179 J/kg K
Dynamic viscosity	$8.55*10^{-4}$ kg/ m s
Water at (60^0 C)Density	983.3 kg/m^3
Thermal conductivity	0.654 W/m.K
Specific heat	4179 J/kg K
Dynamic viscosity	$4.71*10^{-4}$ kg/ m s

Table-2 Items specifications	
I. Name	Item Description
Pipe -1	Plastic pipe, Length = 1.0 m, Inside diameter = 0.0408 m, Wall thickness = 0.00368 m
Pipe-2	Length = 1.0 m,Inside diameter = 0.01579 m, Wall thickness = 0.00276 m
Pipe-3, pipe-4	Length = 0.75 m, Inside diameter = 0.01579 m, Wall thickness = 0.002768 m
Pipe-5, pipe-6	Plastic type N.S 1/5", OD = 0.02145 mm, ID = 0.01537 mm, Wall thickness =0.00278 mm
Elbow-1	1/5" N.S 90^0
Pump	Power 120 W, Max. head 16 m, Max. flow rate 25 lit/min., Rotation 2860 r/min Current 0.55 A
Plug	Iron, 1in diameter
Push	Iron, 1in diameter
Flange	Iron, 1.5 in diameter
Thermocouples	T1,T2,T3, and T4 type k
Ball valve	PVC, 0.5 in diameter
Tank	Iron, 10 L volume

2.3 Grid Independent Convergence (GIC)

In computational analysis, there is an essential role for the mesh quality to reach an accurate result. Therefore, it is necessary to test the mesh size that will be used in the simulation. Six different mesh element sizes are considered in the test as shown in Fig.3. To achieve a mesh-independent simulation, some parameters are considered. Nusselt number and the inlet and outlet temperatures of the PCM and water are monitored for the tested mesh element sizes. It is clear from the figure that the change in the temperatures and Nusselt number becomes stable at mesh number 4. In the current simulation, mesh number 5 with 610955 elements is considered.

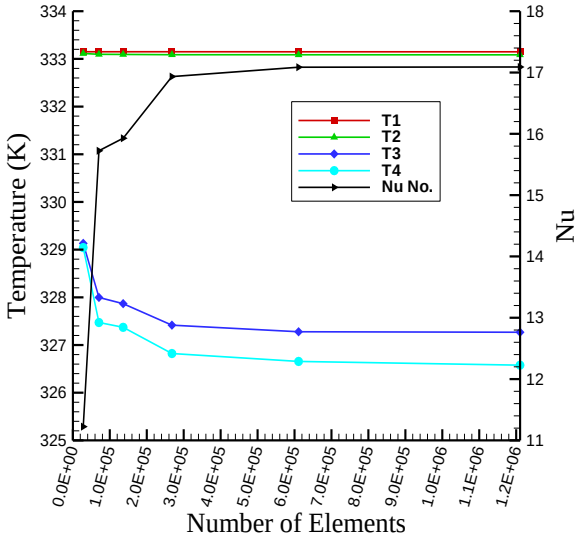

Figure 3. Effect of number of elements in temperature and

3. Experimental procedures

3.1. Experimental Apparatus.

Fig. 4 illustrates the main components of the experimental system with details about the items' specifications as listed in Tab. 2. The main components of the system are elaborated below:

1. Two concentric pipes, the inner steel pipe used for water as the working fluid. Its length is 1.0 m, its inside diameter of 15.79 mm, and its wall thickness of 2.76 mm. The outer shell pipe with an inside diameter of 40.8 mm, and a wall thickness of 3.68 mm. The annulus between the two concentric pipes is filled by 0.8648 kg of paraffin wax as a PCM.
2. The pump is used to circulate the water through the system with a maximum flow rate of 25 L/min.
3. Four thermocouples of type-K are used in the measurements. Two are used for measuring the inlet and outlet water temperatures, and another two are used for measuring the temperature of the PCM in the annulus at the inlet and outlet of the shell pipe.
4. The paraffin wax fills the annulus as a PCM. Its thermophysical properties are listed in Table -1 [14].

5. To reduce the heat losses from the system to the surrounding, the outer wall of the shell pipe was insulated with 2 cm of glass wood.
6. A constant temperature reservoir is used to ensure that the inlet water is maintained at the required temperature with ±0.05C sensitivity. A pump of variable speed achieved the circulation of the hot fluid inside the system. The flow rate of hot fluid was measured by using a variable glass tube sectional area. The thermophysical properties of water, during solidification and melting at 24 ^{0} C and 60 ^{0} C respectively, are listed in Table 3 [15].

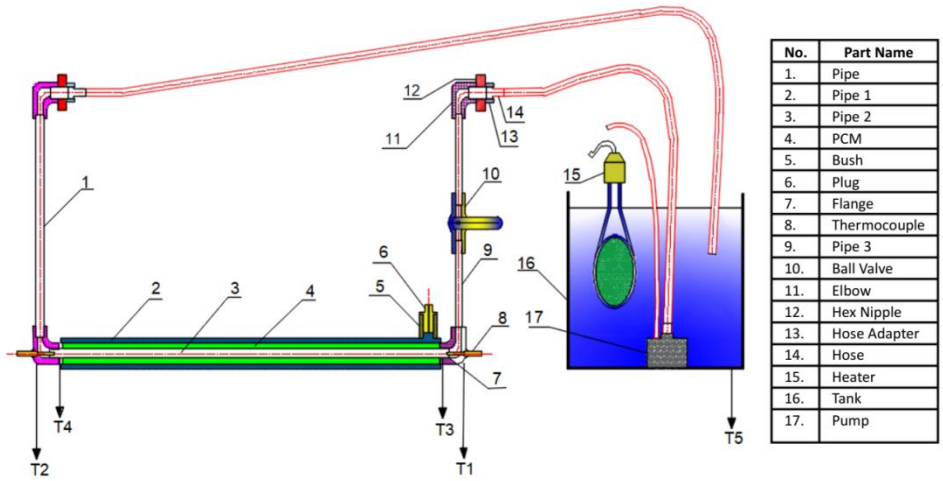

No.	Part Name
1.	Pipe
2.	Pipe 1
3.	Pipe 2
4.	PCM
5.	Bush
6.	Plug
7.	Flange
8.	Thermocouple
9.	Pipe 3
10.	Ball Valve
11.	Elbow
12.	Hex Nipple
13.	Hose Adapter
14.	Hose
15.	Heater
16.	Tank
17.	Pump

Figure 4. Sketch of the experimental rig

3.2. Data Measurement

During the measurements for the charging or melting process, the hot fluid is used for melting the PCM completely at a constant mass flow. Then, the solidification process for cooling the PCM is started. A cold fluid (water) in a constant temperature medium, at 24 °C, is circulated through the tubes for cooling purposes at a constant mass flow rate. The solidification experiment continued till full solidification of the paraffin in the whole domain. The experiments were conducted in the melting state using four different mass flow rates m_1=0.0952 kg/s, m_2=0.0713 kg/s, m_3=0.032 kg/s, and m_4=0.0134 kg/s. The current study will focus on reviewing the findings related to the melting of paraffin wax especially. The temperatures at both boundaries points of the hot fluid and paraffin are precisely acquired.

4. Results and Discussions.

4.1. Experimental Results.

The melting process in the experiments was achieved with approximately 333 K as an inlet water temperature. Four specified mass flow rates were used during running the experiments 0.0952 kg/s, 0.07133 kg/s, 0.032 kg/s, and 0.0134 kg/s. Figs. 5, 6, 7, and 8 show the transient temperature variation at various locations and mass flow rates. The PCM temperatures at the inlet and outlet reach 323 K at 100, 110, 150, and 200 min related to the above mass flow rate respectively. This result indicates that as the mass flow rate increases, the required duration for the paraffin wax to be

completely liquefied decreases. This illustrates an inversely proportional relation between the mass flow rate and the required time for melting. This phenomenon occurs naturally because the heat transfer coefficient increases in forced convection as the Reynolds number rises. This increase is directly related to the fluid velocity through the pipe. which agrees with the results presented in the previous figures. Figs. 9 and 10 provide a clear indication of the periods at which complete melting of paraffin wax occurred that measured at points T3 and T4. The main point in the process of paraffin wax melting is achieving a complete melting within the shortest period by employing the heat of the inlet water flow. Then this heat will be also utilized to heat the outlet water flow during the solidification process.

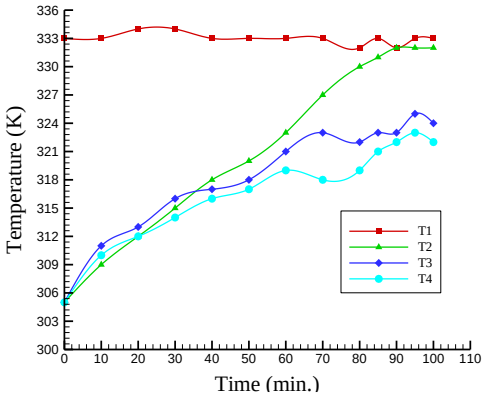

Figure 5 Temperature evolution with time for charging process at m1 = 0.0952 kg/s.

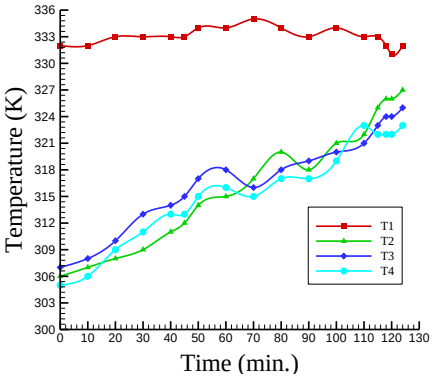

Figure 6 Temperature evolution with time for charging process at m2 = 0.0713 kg/s.

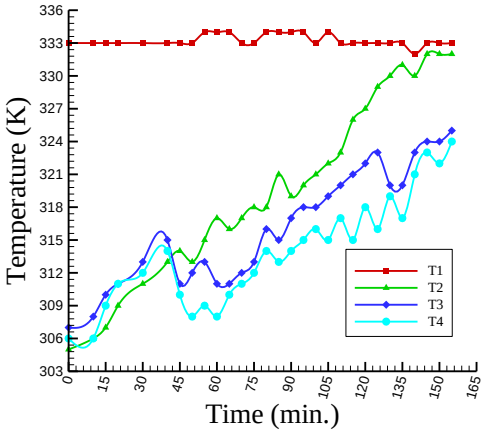

Figure 7 Temperature evolution with time for charging process at m3 = 0.032 kg/s.

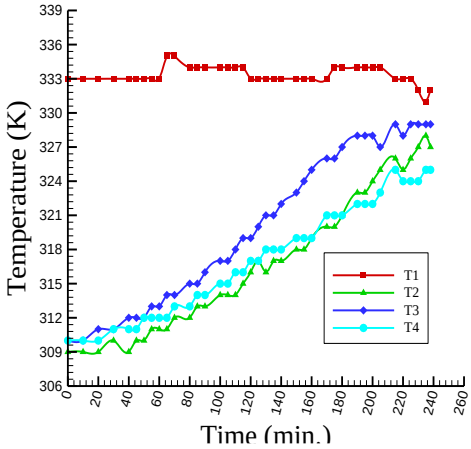

Figure 8 Temperature evolution with time for charging process at m4 = 0.0134 kg/s.

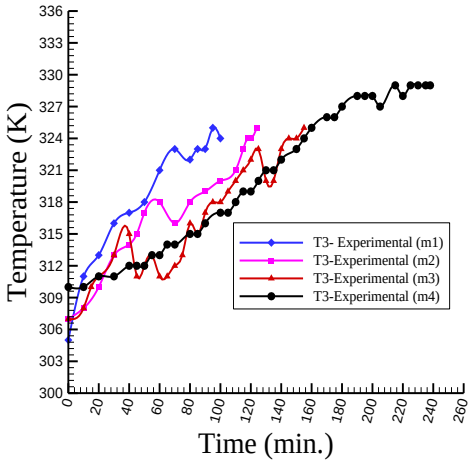

Figure 9 PCM temperature evolution with time for different mass flow rate.

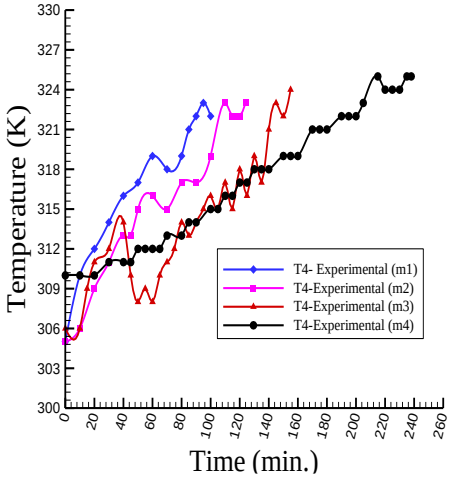

Figure 10 PCM temperature evolution with time for different mass flow rate.

4.2. Parametric Analysis

The numerical results in Figs. 11, 12, and 13 showed that the PCM melting process is completed and its temperature reached the hot working fluid temperature approximately at 110 min as shown in the T3-T4 curves in the above figures. This rate of melting is related to the turbulent flow behavior that occurs for the mass flow rates 0.0952 kg/s, 0.0713 kg/s, and 0.032 kg/s in the numerical solution as the Reynolds number exceeds 2300. This leads to a high heat transfer coefficient during forced convection, resulting in a sufficient heat transfer for melting PCM within a similar period for various mass flows. Fig.14 indicates that the PCM melting temperature reaches the hot working fluid temperature after 160 min., as observed from the results and illustrated by the T3-T4 curves. There is a time difference between T3 and T4 in achieving the required temperature and the complete melting. This delay between them is related to the laminar characteristics of the flow at the mass flow rate of 0.01343 kg/s. Whereas, at Reynolds number less than 2300, the heat transfer coefficient is significantly small compared to the previous case. Hence, it takes a longer time to achieve full PCM melting.

Fig.15 illustrates the liquid friction of melting over time for PCM at different mass flow rates. The results indicate that the transient liquid friction for the first three mass flow rate values are approximately consistent and the complete melting is achieved after 65min. However, when the mass flow rate is under a laminar flow, a longer time is required to achieve complete melting. The numerical productions showed that 90 minutes is the ideal time to achieve a complete melting at a mass flow rate of 0.0134 kg/s. These findings indicate that the latent heat of the phase change material requires a minimum of one hour for the PCM to transfer from a solid to a liquid state. In addition. the process depends on the quantity of PCM added in the annular space between the two tubes and the flow behavior inside the tubes.

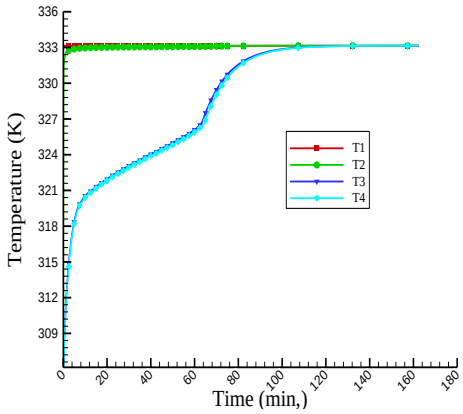

Figure 11 Numerical solution of temperature evolution for charging process at m1= 0.0952 kg/s.

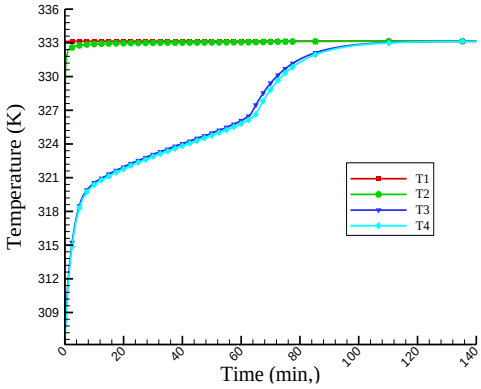

Figure 12 Numerical solution of temperature evolution for charging process at m2= 0.0713 kg/s.

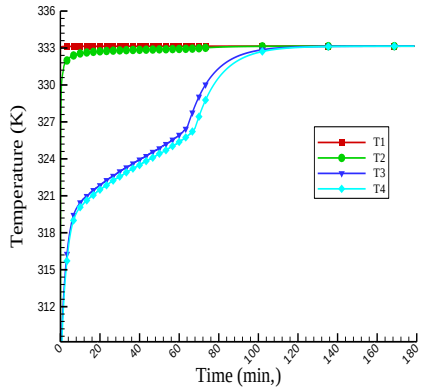

Figure 13 Numerical solution of temperature evolution for charging process at m3= 0.032 kg/s.

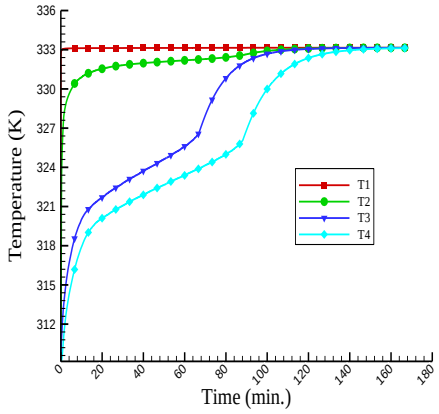

Figure 14 Numerical solution of temperature evolution for charging process at m4 = 0.0134 kg/s.

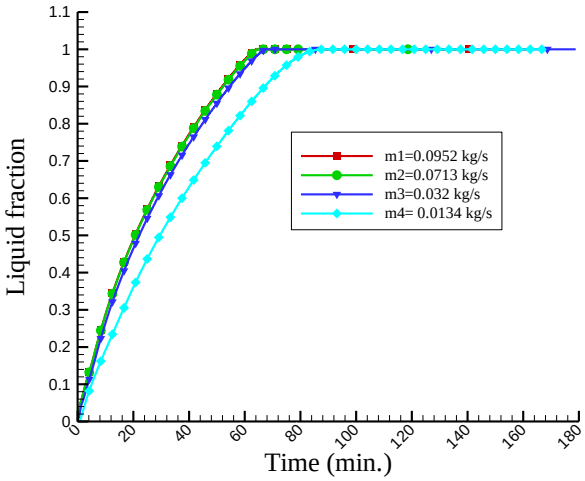

Figure 15 Liquid fractions for different mass flow rate with time.

4.3. Comparison between Model and Experiment

Figs. 16-19 show the measured and predicted values of the local temperature T3 and T4 in the paraffin wax domain. These figures help in observing the mechanism of paraffin wax melting when the hot water flows through the inner tube. The experiments that were used to achieve a complete melted paraffin wax showed different durations depending on the mass flow rate of water. However, the numerical solution indicated nearly consistent durations for complete paraffin wax melting across various mass flow rates of water. This can be associated with the consistent properties of the PCM through the solution, which does not significantly change with temperature variations, as demonstrated by these results. The numerical solution indicated that the PCM reaches 330K at 80 min under all flow rate conditions. These findings showed that the maximum variation between the numerical and practical results, which ranges from 3.4% to 4.8%, is at a mass flow rate of 0.0134 kg/s. This limit of deviation is considered acceptable for comparing theoretical and practical outcomes in this research.

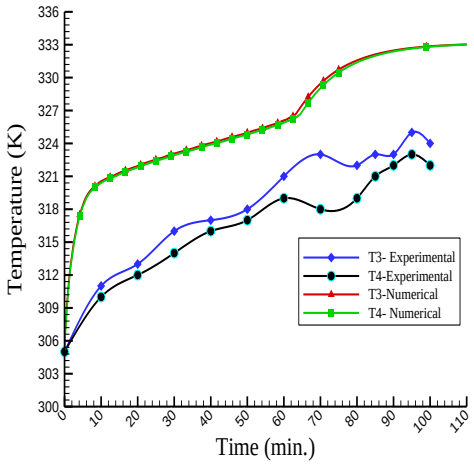

Figure 16 PCM temperature evolution with time for charging process at m1 = 0.0952 kg/s.

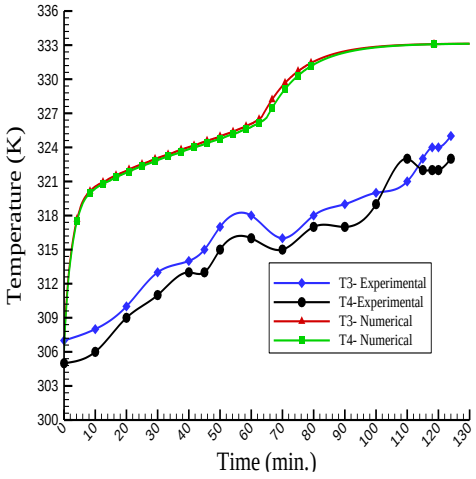

Figure 17 PCM temperature evolution with time for charging process at m2 = 0.0713 kg/s.

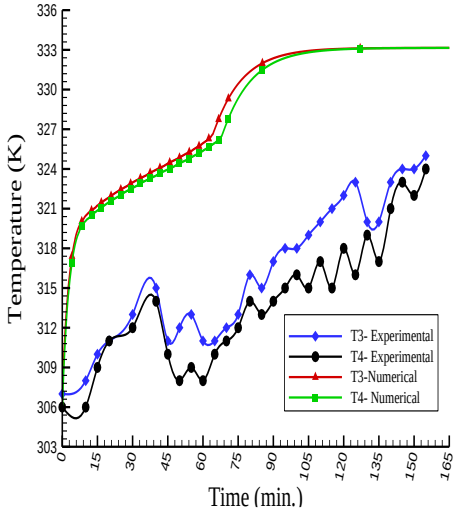

Figure 18 PCM temperature evolution with time for charging process at m3 = 0.032 kg/s.

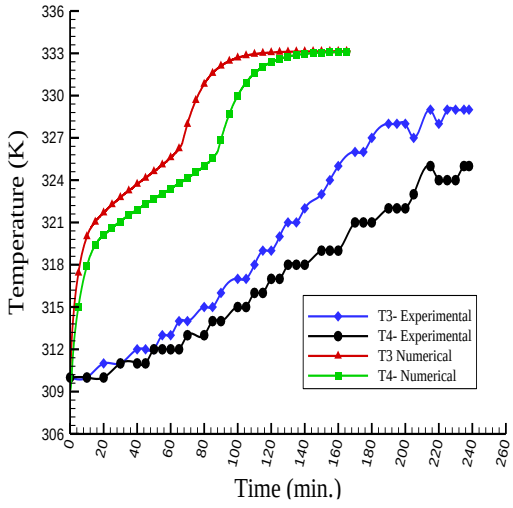

Figure 19 PCM temperature evolution with time for charging process at m4 = 0.0134 kg/s .

5. Conclusion

The present work proposed a numerical and experimental analysis that can predict the behavior of a PCM domain. The PCM was inserted into an annulus formed between an internal iron tube and an outer plastic shell. The PCM works as a latent heat thermal energy storage system during the charging process (melting phase). The novelty of this research is represented by the three-dimensional analysis of the melting process. It has proved to be efficient for describing the behavior of the entire LHTES. Also, it presented variations in the results with various mass flow rates, which consider adiabatic boundary conditions along the shell length. The numerical results were validated through a comparison with the experimental data at a mass flow rate of 0.0134 kg/s, which showed a maximum error of 4.8% and gave 80 min to reach 333 K. The results showed that the paraffin wax at points T3 and T4 transforms into a liquid state at different periods depending on the mass flow of water. Whereas the time of transformation into the liquid state decreases with increasing the amount of flow, as shown in Figures 9 and 10.

References.

[1] Long Jian-you, Numerical and experimental investigation for heat transfer in triplex concentric tube with phase change material for thermal energy storage, *Solar Energy*, 82, (2008), pp 977–985.

[2] Abduljalil A. Al-Abidi, *et al.*, Numerical study of PCM solidification in a triplex tube heat exchanger with internal and external fin, *International Journal of Heat and Mass Transfer*, 61,(2013), pp684–695.

[3] Wei-Wei Wang, *et al.*, Numerical study of the heat charging and discharging characteristics of a shell-and-tube phase change heat storage unit, *Applied Thermal Engineering*,58,(2013), pp 542-553.

[4] M.A. Kibria, *et al.*, Numerical and experimental investigation of heat transfer in a shell and tube thermal energy storage system, *International Communications in Heat and Mass Transfer*, 53, (2014), pp 71-78.

[5] M. K. Rathod, and J. Banerjee, Experimental Investigations On Latent Heat Storage Unit Using Paraffin Wax As Phase Change Material, *Experimental Heat Transfer*, 27, (2014), pp 40–55.

[6] Jaume Gasia, *et al.*, Experimental Evaluation of a Paraffin as Phase Change Material for Thermal Energy Storage in Laboratory Equipment and in a Shell-and-Tube Heat Exchanger, *Applied Sciences*, 6 112, (2016).

[7] Seddegh, S., *et al.*, Investigation of the effect of geometric and operating parameters on thermal behavior of vertical shell-and-tube latent heat energy storage systems, *Energy*,137, (2017), pp69-82.

[8] Guang-Shun Han, *et al.*, A Comparative Study On The Performances Of Different Shell-And-Tube Type Latent Heat Thermal Energy Storage Units Including The Effects Of Natural Convection, *International Communications in Heat and Mass Transfer*, 88, (2017), pp228–235.

[9] Gang Shen *et al.*, Investigation on optimal shell-to-tube radius ratio of a vertical shell-and-tube latent heat energy storage system, *Solar Energy*, 211, (2020),pp732–743.

[10] B A Abbas and M B Al-hadithi, Numerical Prediction of Melting Phenomena of PhaseChange Material in the Annulus of Two Concentric Pipes: Performance and Behavior", *AIP Conference Proceedings 2806*, (2023), pp 080001-1–080001-15.

[11] S.M. Jalil, Mathematical and numerical predictions for optimum perfect mixing by bulk convective oscillatory exchange, *International Journal of Heat and Mass Transfer*, 167, (2021), pp120792 –12.

[12] S. M. Jalil, Phase-lags' radial variations between velocity, shear stress, and pressure gradient in ultrahigh frequency pulsating turbulent flows, *Journal of Fluids Engineering, Transactions of the ASME,* 2020, 142(5), 051201-1.

[13] ANSYS, *ANSYS Fluent Theory Guide*, Release 17.1, ANSYS, 2016. https://www.ansys.com/products/fluids/ansys-fluent.

[14] Mustafa B. Al-Hadithi, Saad M. J. Alazawi, The effect of phase change material on thermal energy storage in cement layers, *Int. J. Nanoelectronics and Materials*, 9, (2016), pp 133-142.

[15] J. P. Holman, *Heat Transfer*, Published by McGraw-Hill Company, 10th ed., (2010).

Paper submitted: 23.01.2024

Paper revised: 24.03.2024

Paper accepted: 08.04.2024